Advances in Differential Equations and Control Processes 2025, 32(4), 3703.
doi: https://doi.org/10.59400/adecp3703

Article

A delay mathematical model to examine control strategies of the coronavirus pandemic with an efficient approach

Awais Ahmad[1], Muhammad Uzair Awan[1], Shah Zeb[2,*], Baboucarr Ceesay[3,*], Muhammad Rafiq[4], Ayesha Kamran[5], Awais Shaukat[4]

[1] Department of Mathematics, Government College University, Faisalabad 38000, Pakistan
[2] School of Distance Education, Universiti Sains Malaysia, Penang 11800, Malaysia
[3] Mathematics Unit, University of The Gambia, Serekunda PO. Box 3530, The Gambia
[4] Department of Mathematics, Namal University, Mianwali 42250, Pakistan
[5] Department of Mathematics, University of Management and Technology, Lahore 54770, Pakistan
*** Corresponding author:** Shah Zeb, shahzeb@student.usm.my; Baboucarr Ceesay, bceesay@utg.edu.gm

CITATION

Ahmad A, Awan MU, Zeb S, et al. A delay mathematical model to examine control strategies of the coronavirus pandemic with an efficient approach. Advances in Differential Equations and Control Processes. 2025; 32(4): 3703. https://doi.org/10.59400/adecp3703

ARTICLE INFO

Received: 19 September 2025
Revised: 8 October 2025
Accepted: 31 October 2025
Available online: 8 November 2025

Abstract: Most of the countries are affected by the COVID-19 disease, with many deaths and infected cases. Coronavirus is a viral disease-causing symptom such as fever or chills, dry cough, shortness of breath, loss of taste or smell, and headache. Since Covid have a significant impact on the public health that is why a delayed pandemic model of coronavirus disease is extended. The study explores the model's aspects, including the positivity, boundedness of the delayed pandemic model, existence and uniqueness. The next-generation matrix approach, which defined whether or not the disease continues in the population, was used to determine the basic reproductive number. The Routh-Hurwitz criterion result, the Jacobian matrix, and the Lyapunov functions are used to explain the system's local and global stability at both disease-free and endemic points. We employ the non-standard finite difference approach, RK-4, and Euler in numerical analysis. We have shown the consistency of analysis and positivity of the model. The non-standard finite difference scheme is more reliable and sufficient as compared to the Forward Euler and RK-4 schemes. Because the non-standard finite difference method showed convergence at a very small step size. The results of the given model are directly applicable to the health sector, since they allow predicting the outbreak pattern and evaluating the efficiency of interventions. Knowing and planning the impact of delay factors and vaccination strategies on the disease dynamics, health authorities may incorporate specific interventions, minimize the infection peaks, and utilize the resources available in the health system without overloading it.

Keywords: basic reproductive number; lyapunov function; global stability; existence and uniqueness; non-standard finite difference

1. Introduction

In 2003, the serious acute respiratory syndrome (SARS) was first identified in Asia [1]. After that, the disease spread to other countries. High body temperature, diarrhea, discomfort, dry cough, and respiratory issues are among the main signs of the SARS virus [2]. It is an airborne illness that is transferred by microscopic droplets released by an infected person when they cough, sneeze, laugh, or speak. Depending on the viral phase, health status, and immunity, these symptoms can range from moderate

to severe [3]. Coronaviruses are members of the Coronaviridae family. These viruses' range between 65 and 125 nm in size. They are single-stranded Ribonucleic acid (RNA) molecules that are 22–26 kilobases in size and have a single nucleus. Alpha α, beta β, gamma γ, and δ viruses are other members of the coronavirus family. Middle East respiratory syndrome and influenza. The most prevalent lung infections that can seriously harm the respiratory system are coronaviruses (MERS-COV) [4]. They could possibly result in lung failure. Because camels, bats, and monkeys were the illness's primary hosts, it was formerly thought to be exclusively an animal sickness. It was later spread to humans, and it is currently a global calamity. discovered the traits, locations, and mode of transmission of the coronavirus in humans [5]. In December 2019, the SARS-CoV-2, or COVID-19, outbreak began in Wuhan, China. The SARS virus and this one were comparable [6]. It is believed that humans contracted COVID-19 from bats. This virus's early symptoms were comparable to those of the pneumonia virus [7]. After spreading around the world, this virus finally made its way to the US on January 20, 2020. On March 11, 2020, it was declared a pandemic by the WHO. The initial value of R_v was around 2.5. It is known as the coronavirus because of its structure, which resembles a crown. The respiratory system's cells are attacked by the spike protein. COVID-19 slowly infiltrates human bodies with its tainted RNA. After then, the virus quickly expands its production and replicates. Although everyone can contract the coronavirus, the elderly and ill are most vulnerable. It can spread quickly among those with weakened immune systems and respiratory conditions. This illness has a higher mortality rate since it might recur in a person. The number of fatalities is rising. Among them, the virus infected 70,000 people in the first 50 days. According to reports, the virus belongs to the beta group of coronaviruses. The United States of America had the highest infection rate in the world, while Vietnam had the lowest and Brazil the highest fatality rate [8]. Influenza A and Influenza B viruses are not the same as COVID-19. Its strain is comparable to SARS-CoV-2, and symptoms start to show up two to fourteen days after the susceptibility. Compared to the other viruses in the family, COVID-19 has been found to be more contagious. After contracting the virus, one may lose their sense of taste or smell. Patients may also experience additional complications, including fever and respiratory disorders. As a result, the significance of taking preventative action against these illnesses has grown. Hand sanitization, face masks, and social isolation can all significantly reduce the dynamics of the disease [9]. Vaccination plays a significant element in disease control. However, there is no guarantee that a vaccinated individual won't develop the virus. Research suggests that individuals with robust immune systems can limit the spread of the illness. The World Health Organization (WHO) estimates that the virus has infected around 30 million individuals globally so far. About one lakh and ninety-four thousand people have been reported dead, whereas seven lakh and sixty-five thousand people have been reported recovered. Two hundred thirty-seven fatalities and 11,000 carriers of 2019-Cov have been recorded in Pakistan. Regretfully, only 2% of testing kits and lab equipment are readily available. Therefore, delay techniques, like travel restrictions, self-quarantine, and social isolation, were put into place by policymakers to manage the global pandemic. The World Health Organization (WHO) has declared the 2019-nCov

pandemic to be a worldwide concern [10]. In 2021, Ahmed et al. used the SEQIIR model to investigate the coronavirus's behavior. To gain a deeper understanding of the illness phenomenon, they employed ODE and FDE models [11]. Similarly, Hassan et al. proposed the SIIR compartmental model in 2021 to study the illness waves in Texas, USA [12].

In order to observe the dynamics of COVID-19 in the Kingdom of Saudi Arabia, Alqarni et al. presented the DSIARB epidemic model [13]. Similar to this, Savi and his colleagues investigated an SEIRDC epidemic model in Brazil to assess the virus's spread [14]. Tiwari et al. investigated how quarantine affected the disease's dynamics in India. They examined the SEIRD model to investigate the illness dispersion [15]. In 2021, Warbhe et al. examined a SIRM model to investigate the financial damages brought on by COVID-19. Daniel investigated the kinetics of the COVID-19 infection with the diffusion process in 2021 using the compartmental (SEIQCRW) model [16]. When evaluating the sizes, peaks, and transmission patterns of an infectious illness like the new SARS-CoV-2, mathematical modeling is helpful and appropriate. It is crucial to run the influencing parameters of any infectious disease pandemic into a mathematical testing model in order to take further precautions. From the traditional SIR to more complex models, there are several mathematical representations of infectious illnesses, including compartmental models. These models are crucial for quantifying potential mitigation and control measures for infectious diseases. Numerous aspects of the illness have been examined using mathematical modeling [17], which can also offer the means to forecast the patterns of transmission dynamics of a communicable illness like COVID-19. When assessing the momentum of disease outbreaks and implementing public health measures, mathematical models that estimate disease progression might be useful [18].

By adding delay variables to the differential equation system, the mathematical modeling of the coronavirus closely resembles the actual phenomenon. The specified reproduction number plays a crucial part in this study in explaining the nonlinear dynamics of biological engineering as well as several other physical nonlinear issues. The control of 2019-Cov is indicated if the reproduction number is fewer than one. A reproduction number higher than one, on the other hand, suggests that 2019-nCov has been steadily rising. In this model, we have incorporated the delay factor. Delay considerations include things like quarantine, isolated location, vaccination, etc. Our problem is an initial value problem, as shown by the negative sign with μ, which moves toward initial values when the delay term is applied [19]. To this end, we have included a τ rate factor that can slow the spread of sickness. In typical epidemiological models, the illness converges toward stable locations if the infection rate is kept under control. Since infection control is currently almost unachievable, delaying measures including social separation, isolation, and quarantine are being used to combat the 2019 COVID-19 pandemic. Fortunately, the delay factors or delaying tactics used in the simulation are independent of the kind of transmission rate. Our research indicates that NSFD with time delay is being used for the first time to explore this model. A trustworthy numerical analysis that maintains all the essential characteristics is necessary to examine the precise behaviors of such a model. NSFD shows convergence

at a very small step size, and this method is more reliable for other models with vaccination, like Rubella and Covid [20, 21]. Using methods like Euler, RK4, and especially NSFD with this model improves its accuracy and stability, making long-term predictions about coronavirus more reliable [22]. This comparison offers important insights into the model's practical applicability and can guide future research on choosing appropriate numerical methods for similar systems [23–26].

This paper presents an extended version of the epidemic model of Corona virus. We apply a delay factor on this model, by converting a simple model to a delay system. Among the contributions of the new methodology approach, this includes that some factors have positive sensitivity indices and others show negative sensitivity. Mathematically, to do stability analysis or control analysis, it is necessary to prove that the system under study has a well-defined solution. Establishing the existence and uniqueness means that the model is consistent in its behaviour under specified initial conditions and the value of parameters, and the findings of stability analysis are non-meaningless. This paper further explores the new graphs of different effects of tau on its own different values and it presents the 3D graph of the difference between the reproductive number, gamma function, and beta function; and it further analyze the graph at different values of (S). This work offers the new extension to existing coronavirus models, firstly, this study is based on the analysis of a delay model, and it examine the critical behavior of delay rate and reproductive number. Finally, it highlights the impact on epidemic control strategies.

The paper's methodology is as follows: Section 1 is an overview of the literature on conditions that have a brief history and are comparable to coronavirus. Section 2 discusses the formulation and mathematical analysis of the delayed model, model analysis, model equilibrium point, reproduction number and also discusses the local and global stability and sensitivity analysis of parameters. We describe the convergence of our NSFD technique, Consistency Analysis, present numerical experiments at various stages, and show the outcomes of our numerical simulations in Section 3. In Section 4, we discuss the conclusions.

2. Methods and materials

2.1. Delay mathematical model

In order to combat the deadly coronavirus illness, delay modeling is a crucial task. We know that by using delay methods on humans, we may lower the incidence of coronavirus illness. Although it will take time, we may prevent infectious illnesses by adhering to certain guidelines. We utilized interventional measures between susceptible and infected persons using a model that we obtained from Saleem et al. [2]. Since all necessary information is provided in the compartmental information below, the model formulation is simple to understand. As previously said, we employ several divisions in this situation. **Figure 1** demonstrates the Coronavirus delay model.

- S(t) describes the susceptible class.
- I(t) demonstrate the Infected class.
- V(t) describes the vaccinated class.

- R(t) describe the recovered class.

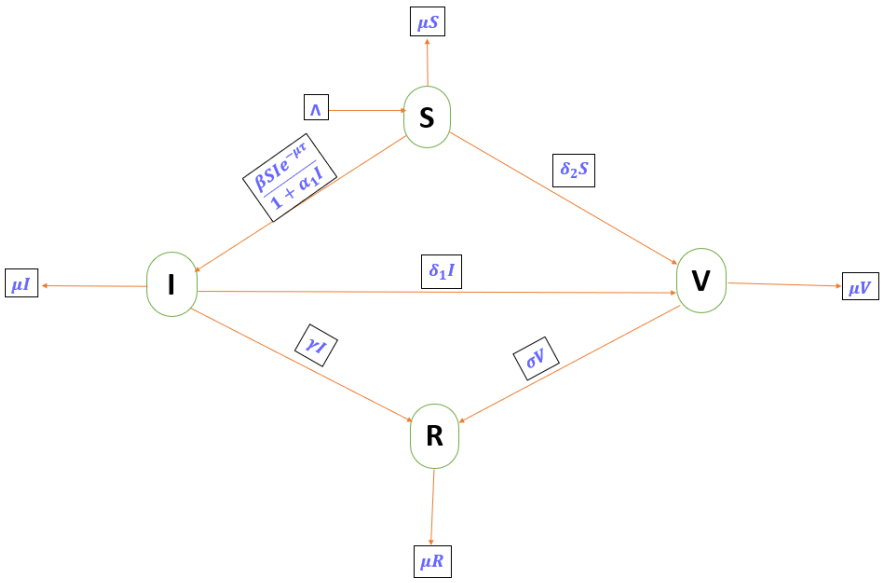

Figure 1. Flow chat of Coronavirus delay model.

The susceptible humans of size S(t), the infected individual population of size I(t), Vaccinated humans of size V(t), and the recovered humans of size R(t) make up the host population of size N(t), which is

$$N(t) = S(t) + I(t) + V(t) + R(t). \tag{1}$$

Depending on variables like recruitment or the susceptible population's birth rate, Λ is the rate at which a new population joins the vulnerable category. Disease is transmitted at a rate of β from the susceptible compartment to the infected in the compartment through direct contact with infectious persons. μ represents the vulnerable class's natural death rate. The population's crowding impact on the virus is $\frac{1}{(1+\alpha_1 I)}$. Consequently, the differential equation that follows explains the total rate of change of vulnerable individuals:

$$\frac{dS}{dt} = \Lambda - \frac{\beta S I e^{-\mu\tau}}{1+\alpha_1 I} - (\delta_2 + \mu)\, S.$$

The delayed direct transmission of the illness in the infected compartment is taken into consideration by $e^{-\mu\tau}$ in the exposed class. The rate at which the infected population received vaccinations during the quarantine or isolation period is denoted by the phrase δ_1. The natural death rates of the afflicted population are denoted by μ. The following differential equation controls the rate of change of the infected human population I(t):

$$\frac{dI}{dt} = \frac{\beta S I e^{-\mu\tau}}{1+\alpha_1 I} - (\delta_1 + \mu + \gamma)\, I.$$

The rate of doses in the population who recovered or got immune after vaccination is σ. The overall change of vaccinated population is denoted by the following

differential equation:

$$\frac{dV}{dt} = \delta_2 S + \delta_1 I - (\sigma + \mu)V.$$

The force of infection of virous is βI. The rate at which infected population may recover due to its internal immunity and natural circumstances. The change of recovered population is denoted by the differential equation:

$$\frac{dR}{dt} = \gamma I + \sigma V - \mu R.$$

The individuals who recovered from the Vaccinated were transferred to class R(t). The parametric dimensions shown in **Table 1** below were used to conduct numerical and graphical analyses for this model.

Table 1. Values of parameters used in the SIVR COVID-19 model.

Parameter	Description	Values/per day	Reference
Λ	Recruitment rate of population	0.02537	Estimated
β	Transmission rate of infection	0.4000	Saleem et al. [2]
γ	Recovery rate of infected	0.5000	Saleem et al. [2]
μ	Natural death rate	0.00004046	Saleem et al. [2]
α_1	Vaccination-related parameter	0.5465	Saleem et al. [2]
δ	General removal rate	0.5000	Saleem et al. [2]
δ_1	Population got vaccinated	0.1000	Saleem et al. [2]
δ_2	Susceptible population got vaccinated	5.32978	Saleem et al. [2]
σ	Population who recovered or got immune after vaccination	$\geq$0	Saleem et al. [2]
τ	Time delay	$\geq$0	Assumed

The System of delay differential equation for the given mathematical model

$$\begin{aligned}
\frac{dS}{dt} &= \Lambda - \frac{\beta S I e^{-\mu\tau}}{1+\alpha_1 I} - (\delta_2 + \mu)\, S, \\
\frac{dI}{dt} &= \frac{\beta S I e^{-\mu\tau}}{1+\alpha_1 I} - (\delta_1 + \mu + \gamma)\, I, \\
\frac{dV}{dt} &= \delta_2 S + \delta_1 I - (\sigma + \mu)V, \\
\frac{dR}{dt} &= \gamma I + \sigma V - \mu R,
\end{aligned} \tag{2}$$

With initial conditions

$$S \geq 0, \quad I \geq 0, \quad V \geq 0, \quad R \geq 0.$$

Here, t ≥ 0. $\tau \leq t$.

2.2. Model analysis

In this Part, we calculate a conceptual analysis of the dynamic's behavior of coronavirus disease. This analysis consists of model properties such as the positivity, model equilibrium states, and boundedness of solution.

Theorem 1. *The proposed model of disease possesses a non-negative solution,*

providing nonnegative initial conditions for all $t \geq 0$.

Proof of Theorem 1. It is clear from the system of equation

$$\begin{aligned} \left.\frac{dS}{dt}\right|_{S=0} &= \Lambda \geq 0, \\ \left.\frac{dI}{dt}\right|_{I=0} &= 0, \\ \left.\frac{dV}{dt}\right|_{V=0} &= \delta_2 S + \delta_1 I \geq 0, \\ \left.\frac{dR}{dt}\right|_{R=0} &= \gamma I + \sigma V \geq 0. \end{aligned} \tag{3}$$

Which shows that positivity exists in the system with initial conditions. □

Theorem 2. *Solution of the equations are all bounded in probable region* ω.

Proof of Theorem 2. The total population is $N(t)$ and the Sum of all the differential equations:

$$\frac{dN}{dt} = \frac{dS}{dt} + \frac{dI}{dt} + \frac{dV}{dt} + \frac{dR}{dt}.$$

Substituting the right-hand sides of the equations, we get:

$$\frac{dN}{dt} = \Lambda - \mu\left(S(t), I(t), V(t), R(t)\right),$$

This implies that,

$$\frac{dN}{dt} = \Lambda - \mu N(t),$$

This is a linear differential equation. To solve the variables and integrate them:

$$\int \frac{dN}{\Lambda - \mu N} = \int dt,$$

After integration we obtain:

$$-\frac{1}{\mu}\ln(\Lambda - \mu N) = t + A,$$

Taking Exponential on both sides:

$$\Lambda - \mu N = Ae^{-\mu t},$$

Solving for N(t), we find:

$$N(t) = \frac{\Lambda}{\mu} + \left(N(0) - \frac{\Lambda}{\mu}\right)e^{-\mu t}.$$

As $t \to \infty$, the exponential term $e^{-\mu t} \to 0$, implying:

$$N(t) \to \frac{\Lambda}{\mu}.$$

Thus, N(t) $\leq \frac{\Lambda}{\mu}$ for all t ≥ 0. Therefore, whole population N(t) is bounded and satisfies $0 < N(t) \leq \frac{\Lambda}{\mu}$. This ensures that all solutions remain within efficient region ω:

$$\omega = [(S(t), I(t), V(t), R(t)) \in R_+^4 \mid 0 < N(t) \leq \frac{\Lambda}{\mu}].$$

□

2.3. Model equilibrium points

The system has two different forms of equilibrium, indicated by ϵ_0 and ϵ_1, which stand for disease-free and endemic equilibrium points.

2.3.1. Disease free equilibrium point

The disease-free equilibrium points are:

$$\epsilon_0 = (S_0, I_0, V_0, R_0) = \left(\frac{\Lambda}{\delta_2 + \mu}, 0, 0, 0\right).$$

2.3.2. Reproduction number

The system's dynamics are examined using the basic reproductive number. The predicted number of secondary cases that a typical infected individual could produce in a completely susceptible group throughout the infectious period is known as R_0. We have the reproductive number with R_0 in our situation. This quantity serves as a cutoff point for determining whether a disease will spread or vanish from the population. The next generation matrix approach may be used to ascertain it. In this method, I stands for the infected population, whereas S, R, and V stand for the population without infection compartments [27]. The fresh rate of infection formation and the rate of stage changeover are described by the two matrices [28], F and V, respectively.

We are currently approaching the system with the next-generation matrix method. The transmission and transition matrices are used in this section to compute the reproduction number. For the next generation matrix method.

We maintain the condition for the reproductive number. We used the same classes as those described in Saleem et al. [2]. Then we calculate our reproductive number with the time delay parameter because the classes cannot be changed. So, we maintain the classes.

$$\frac{dx}{dt} = f(x, y) - v(x, y),$$

$$F = \begin{bmatrix} \frac{\beta S I e^{-\mu\tau}}{1+\alpha_1 I} \\ 0 \\ 0 \end{bmatrix}, \qquad V = \begin{bmatrix} (\delta_1 + \mu + \gamma) I \\ -\delta_2 S - \delta_1 I + (\sigma + \mu) V \\ -\gamma I - \sigma V + \mu R \end{bmatrix},$$

After at the Disease-free points, both transmission matrix F and V are:

$$\mathcal{F} = \begin{bmatrix} \frac{\beta \Lambda e^{-\mu\tau}}{\delta_2+\mu} & 0 & 0 \\ 0 & 0 & 0 \\ 0 & 0 & 0 \end{bmatrix}, \qquad \mathcal{V} = \begin{bmatrix} \delta_1 + \mu + \gamma & 0 & 0 \\ -\delta_1 & \sigma + \mu & 0 \\ -\gamma & -\sigma & \mu \end{bmatrix},$$

$$\mathcal{F}\mathcal{V}^{-1} = \begin{bmatrix} \frac{\beta\Lambda e^{-\mu\tau}}{(\delta_2+\mu)(\delta_1+\mu+\gamma)} & \frac{\beta\delta_1\Lambda e^{-\mu\tau}}{(\delta_2+\mu)(\sigma+\mu)(\delta_1+\mu+\gamma)} & \frac{\beta\Lambda(\delta_1\sigma+\sigma\gamma+\mu\gamma)e^{-\mu\tau}}{\mu(\delta_2+\mu)(\sigma+\mu)(\delta_1+\mu+\gamma)} \\ 0 & 0 & 0 \\ 0 & 0 & 0 \end{bmatrix}.$$

$\mathfrak{R}_0$ is the spectral radius of $\mathcal{F}\mathcal{V}^{-1}$.

Mathematically,

$$\mathfrak{R}_0 = \frac{\beta\Lambda e^{-\mu\tau}}{(\delta_2+\mu)(\delta_1+\mu+\gamma)}.$$

2.3.3. Endemic equilibrium point

The endemic equilibrium points are:

$$\epsilon_1 = (S_1, I_1, V_1, R_1) = (S^*, I^*, V^*, R^*).$$

This implies that,

$$\begin{aligned} S^* &= \frac{\Lambda(1+\alpha_1 I)}{\beta I e^{-\mu\tau} + (\delta_2+\mu)(1+\alpha_1 I)}, \\ I^* &= \frac{\beta S^* e^{-\mu\tau} - \delta_1 - \mu - \gamma}{\delta_1\alpha_1 + \alpha_1\mu + \alpha_1\gamma}, \\ V^* &= \frac{\delta_2 S^* + \delta_1 I^*}{\sigma+\mu}, \\ R^* &= \frac{\gamma I^* + \sigma V^*}{\mu}. \end{aligned}$$

2.4. Stability analysis

In this section, we determine the local and global stability of the system at disease free and endemic equilibrium.

Theorem 3. *The system at* $\epsilon_0 = (S_0, I_0, V_0, R_0) = \left(\frac{\Lambda}{\delta_2+\mu}, 0, 0, 0\right)$ *is locally asymptotically stable if* $\mathfrak{R}_0 < 1$.

Proof of Theorem 3.

$$J = \begin{bmatrix} -\frac{\beta I e^{-\mu\tau}}{1+\alpha_1 I} - \delta_2 - \mu & -\frac{\beta S e^{-\mu\tau}}{(1+\alpha_1 I)^2} & 0 & 0 \\ \frac{\beta I e^{-\mu\tau}}{1+\alpha_1 I} & \frac{\beta S e^{-\mu\tau}}{(1+\alpha_1 I)^2} - \delta_1 - \mu - \gamma & 0 & 0 \\ \delta_2 & \delta_1 & -(\sigma+\mu) & 0 \\ 0 & \gamma & \sigma & -\mu \end{bmatrix}$$

At disease free point the Jacobian matrix is,

$$J(\epsilon_0) = \begin{bmatrix} -\delta_2 - \mu & -\frac{\beta\Lambda e^{-\mu\tau}}{\delta_2+\mu} & 0 & 0 \\ 0 & \frac{\beta\Lambda e^{-\mu\tau}}{\delta_2+\mu} - \delta_1 - \mu - \gamma & 0 & 0 \\ \delta_2 & \delta_1 & -(\sigma+\mu) & 0 \\ 0 & \gamma & \sigma & -\mu \end{bmatrix}$$

Consider $|J\epsilon_0 - \lambda I| = 0$, and here

$$\begin{vmatrix} -\delta_2 - \mu - \lambda & -\frac{\beta\Lambda e^{-\mu\tau}}{\delta_2+\mu} & 0 & 0 \\ 0 & \frac{\beta\Lambda e^{-\mu\tau}}{\delta_2+\mu} - \delta_1 - \mu - \gamma - \lambda & 0 & 0 \\ \delta_2 & \delta_1 & -(\sigma+\mu) - \lambda & 0 \\ 0 & \gamma & \sigma & -\mu - \lambda \end{vmatrix} = 0$$

Solving the determinant, we get

$$\lambda_1 = -(\delta_2 + \mu) < 0, \quad \lambda_2 = \frac{\beta\Lambda e^{-\mu\tau}}{\delta_2 + \mu} - \delta_1 - \mu - \gamma < 0,$$
$$\lambda_3 = -(\sigma + \mu) < 0, \quad \lambda_4 = -\mu < 0$$

After that,

$$\frac{\beta\Lambda e^{-\mu\tau}}{(\delta_2 + \mu)(\delta_1 + \mu + \gamma)} < 1.$$

This implies that,

$$\mathfrak{R}_0 < 1$$

Consequently, the system is locally asymptotically stable at ϵ_0 when $\mathfrak{R}_0 < 1$ prove. □

Theorem 4. *The system at* $\epsilon_1 = (S_1, I_1, V_1, R_1) = (S^*, I^*, V^*, R^*)$ *is locally asymptotically stable if* $\epsilon_0 > 1$.

Proof of Theorem 4. The Jacobian matrix at ϵ_1 of the system as follows.

$$J = \begin{bmatrix} -\frac{\beta I^* e^{-\mu\tau}}{1+\alpha_1 I^*} - \delta_2 - \mu & -\frac{\beta S^* e^{-\mu\tau}}{(1+\alpha_1 I^*)^2} & 0 & 0 \\ \frac{\beta I^* e^{-\mu\tau}}{1+\alpha_1 I^*} & \frac{\beta S^* e^{-\mu\tau}}{(1+\alpha_1 I^*)^2} - \delta_1 - \mu - \gamma & 0 & 0 \\ \delta_2 & \delta_1 & -(\sigma+\mu) & 0 \\ 0 & \gamma & \sigma & -\mu \end{bmatrix}$$

Consider $|J - \lambda I| = 0$, we get

$$\begin{vmatrix} -\frac{\beta I^* e^{-\mu\tau}}{1+\alpha_1 I^*} - \delta_2 - \mu - \lambda & -\frac{\beta S^* e^{-\mu\tau}}{(1+\alpha_1 I^*)^2} & 0 & 0 \\ \frac{\beta I^* e^{-\mu\tau}}{1+\alpha_1 I^*} & \frac{\beta S^* e^{-\mu\tau}}{(1+\alpha_1 I^*)^2} - \delta_1 - \mu - \gamma - \lambda & 0 & 0 \\ \delta_2 & \delta_1 & -(\sigma+\mu) - \lambda & 0 \\ 0 & \gamma & \sigma & -\mu - \lambda \end{vmatrix} = 0$$

After solving the determinant,

$$\lambda_1 = -\mu < 0, \quad \lambda_2 = -(\sigma + \mu) < 0.$$

$$\lambda^2 + B_1\lambda + B_0 = 0.$$

Where,

$$B_1 = \frac{\beta I^* e^{-\mu\tau}}{1+\alpha_1 I^*} - \frac{\beta S^* e^{-\mu\tau}}{\left(1+\alpha_1 I^*\right)^2} + \delta_1 + 2\mu + \gamma + \delta_2.$$
$$B_0 = (\gamma + \delta_1 + \mu)\left(\frac{\beta I^* e^{-\mu\tau}}{1+\alpha_1 I^*} + \delta_2 + \mu\right) - \frac{(\delta_2+\mu)\,\beta S^*}{\left(1+\alpha_1 I^*\right)^2}.$$

Since B_1, B_0 both are positive when $\mathfrak{R}_0 > 1$, by the Routh-Hurwitz criteria for second order polynomial, the system (1) is locally asymptotically stable at ϵ_1 when $\mathfrak{R}_0 > 1$ as desired. □

Theorem 5. *The system at* $\epsilon_0 = (S_0, I_0, V_0, R_0) = \left(\frac{\Lambda}{\delta_2+\mu}, 0, 0, 0\right)$ *is globally asymptotically stable if* $\mathfrak{R}_0 < 1$.

Proof of Theorem 5. We use a Volterra-type Lyapunov function [29] V: $[0,\infty) \to R$

$$V = S - S_0 \ln S + I + V + R.$$

Taking the time derivative of V

$$V = \left(1 - \frac{S_0}{S}\right) S + I + V + \dot{R}.$$

By putting the derivative,

$$\begin{aligned}
V &= \left(1 - \frac{S_0}{S}\right)\left[\Lambda - \frac{\beta S I e^{-\mu\tau}}{1+\alpha_1 I} - (\delta_2+\mu)\,S\right] + \left[\frac{\beta S I e^{-\mu\tau}}{1+\alpha_1 I} - (\delta_1+\mu+\gamma)\,I\right] \\
&\quad + [\delta_2 S + \delta_1 I - (\sigma+\mu)V] + [\gamma I + \sigma V - \mu R], \\
V &= \left(1 - \frac{S_0}{S}\right)\left[\Lambda - \left(\frac{\beta I e^{-\mu\tau}}{1+\alpha_1 I} + \delta_2 + \mu\right) S\right] + (\delta_1+\mu+\gamma)\left[\frac{\beta S e^{-\mu\tau}}{(1+\alpha_1 I)\,(\delta_1+\mu+\gamma)} - 1\right] I \\
&\quad - (\sigma+\mu)\left[V - \frac{\delta_2 S + \delta_1 I}{\sigma+\mu}\right] - \mu\left[R - \frac{\gamma I + \sigma V}{\mu}\right], \\
V &= \left(\frac{S-S_0}{S}\right)\left(\Lambda - \frac{\Lambda S}{S_0}\right) + (\delta_1+\mu+\gamma)\left(\frac{\beta S e^{-\mu\tau}}{(1+\alpha_1 I)\,(\delta_1+\mu+\gamma)} - 1\right) I \\
&\quad - (\sigma+\mu)\left(V - \frac{\delta_2 S + \delta_1 I}{\sigma+\mu}\right) - \mu\left(R - \frac{\gamma I + \sigma V}{\mu}\right), \\
V &= -\frac{\Lambda\,(S-S_0)^2}{S S_0} + (\delta_1+\mu+\gamma)\left(\frac{\beta \Lambda e^{-\mu\tau}}{(\delta_2+\mu)\,(\delta_1+\mu+\gamma)} - 1\right) I \\
&\quad - (\sigma+\mu)\left(V - \frac{\delta_2 S + \delta_1 I}{\sigma+\mu}\right) - \mu\left(R - \frac{\gamma I + \sigma V}{\mu}\right).
\end{aligned}$$

So, $\dot{V} \le 0$ for $\mathfrak{R}_0 < 1$.

Therefore, the system is globally asymptotically stable at ϵ_1. □

Theorem 6. *The system at* $\epsilon_1 = (S^*, I^*, V^*, R^*)$ *is globally asymptotically stable if* $\mathfrak{R}_0 > 1$.

Proof of Theorem 6. To prove this theorem, we consider the previously constructed Lyapunov function at ϵ_1 as:

$$V = Y_1 \left(S - S^* \ln S\right) + Y_2 \left(I - I^* \ln I\right) + Y_3 \left(V - V^* \ln V\right) + Y_4 \left(R - R^* \ln R\right),$$

Where Y_1, Y_2, Y_3, and Y_4 are constants to be determined afterward

$$V = Y_1 \left(1 - \frac{S^*}{S}\right) S + Y_2 \left(1 - \frac{I^*}{I}\right) I + Y_3 \left(1 - \frac{V^*}{V}\right) V + Y_4 \left(1 - \frac{R^*}{R}\right) R,$$

By putting the value of the derivative of the equations

$$\begin{aligned} V = Y_1 \left(1 - \frac{S^*}{S}\right) \left(\Lambda - \frac{\beta S I e^{-\mu\tau}}{1 + \alpha_1 I} - (\delta_2 + \mu) S\right) + Y_2 \left(1 - \frac{I^*}{I}\right) \left(\frac{\beta S I e^{-\mu\tau}}{1 + \alpha_1 I} - (\delta_1 + \mu + \gamma) I\right) \\ + Y_3 \left(1 - \frac{V^*}{V}\right) (\delta_2 S + \delta_1 I - (\sigma + \mu) V) + Y_4 \left(1 - \frac{R^*}{R}\right) (\gamma I + \sigma V - \mu R), \end{aligned}$$

After simplification,

$$\begin{aligned} V = Y_1 \left(S - S^*\right) \left(\frac{\Lambda}{S} - \frac{\beta I e^{-\mu\tau}}{1 + \alpha_1 I} - (\delta_2 + \mu)\right) + Y_2 (I - I^*) \left(\frac{\beta S e^{-\mu\tau}}{1 + \alpha_1 I} - (\delta_1 + \mu + \gamma)\right) \\ + Y_3 \left(V - V^*\right) \left(\frac{\delta_2 S}{V} + \frac{\delta_1 I}{S} - (\sigma + \mu)\right) + Y_4 \left(R - R^*\right) \left(\frac{\gamma I}{R} + \frac{V}{R} - \mu\right). \end{aligned}$$

Since,

$$\epsilon_1 = (S^*, I^*, V^*, R^*)$$
$$\frac{dS^*}{dt} = \frac{dI^*}{dt} = \frac{dV^*}{dt} = \frac{dR^*}{dt} = 0.$$

Hence,

$$\begin{aligned} (\delta_2 + \mu) &= \frac{\Lambda}{S} - \frac{\beta I e^{-\mu\tau}}{1 + \alpha_1 I}, \quad (\delta_1 + \mu + \gamma) = \frac{\beta S e^{-\mu\tau}}{1 + \alpha_1 I} \\ (\sigma + \mu) &= \frac{\delta_2 S}{V} + \frac{\delta_1 I}{S}, \quad \mu = \frac{\gamma I}{R} + \frac{V}{R} \end{aligned}$$

So,

$$\begin{aligned} V = Y_1 \left(S - S^*\right) \left(\frac{\Lambda}{S} - \frac{\beta I e^{-\mu\tau}}{1 + \alpha_1 I} - \left(\frac{\Lambda}{S} - \frac{\beta I e^{-\mu\tau}}{1 + \alpha_1 I}\right)\right) + Y_2 (I - I^*) \left(\frac{\beta S e^{-\mu\tau}}{1 + \alpha_1 I} - \left(\frac{\beta S e^{-\mu\tau}}{1 + \alpha_1 I}\right)\right) \\ + Y_3 \left(V - V^*\right) \left(\frac{\delta_2 S}{V} + \frac{\delta_1 I}{S} - \left(\frac{\delta_2 S}{V} + \frac{\delta_1 I}{S}\right)\right) + Y_4 \left(R - R^*\right) \left(\frac{\gamma I}{R} + \frac{V}{R} - \left(\frac{\gamma I}{R} + \frac{V}{R}\right)\right). \end{aligned}$$

$$Y_1 = Y_2 = Y_3 = Y_4 = 1.$$

We get, $V = -\frac{\Lambda (S - S^*)^2}{S S^*} \leq 0$, where, $\mathfrak{R}_0 > 1$.

Consequently, the system is globally asymptotically stable at endemic equilibrium point ϵ_1. □

2.5. Sensitivity analysis of parameters

We can calculate the Partial derivative of reproductive number with respect to each parameter of the model to determine the change in reproductive number is negative or

positive for each parameter. We are describing the general formula of the sensitivity analysis and partial derivative of the parameters [30,31].

$$Sensitivity\ Analysis = \frac{\partial \Re_0}{\partial P} \times \frac{P}{\Re_0}$$

Positive effect on $\Re_0$:

$$\frac{\partial \Re_0}{\partial \beta} = \frac{\Lambda e^{-\mu\tau}}{(\delta_2+\mu)(\delta_1+\mu+\gamma)} > 0 \quad \text{(positive effect)}$$

$$\frac{\partial \Re_0}{\partial \Lambda} = \frac{\beta e^{-\mu\tau}}{(\delta_2+\mu)(\delta_1+\mu+\gamma)} > 0 \quad \text{(positive effect)}$$

Negative effect on $\Re_0$:

$$\frac{\partial \Re_0}{\partial \delta_1} = -\frac{\beta\Lambda e^{-\mu\tau}}{(\delta_2+\mu)(\delta_1+\mu+\gamma)^2} < 0 \quad \text{(negative effect)}$$

$$\frac{\partial \Re_0}{\partial \delta_2} = -\frac{\beta\Lambda e^{-\mu\tau}}{(\delta_2+\mu)^2(\delta_1+\mu+\gamma)} < 0 \quad \text{(negative effect)}$$

$$\frac{\partial \Re_0}{\partial \gamma} = -\frac{\beta\Lambda e^{-\mu\tau}}{(\delta_2+\mu)(\delta_1+\mu+\gamma)^2} < 0 \quad \text{(negative effect)}$$

$$\frac{\partial \Re_0}{\partial \mu} = -\frac{\beta\Lambda e^{-\mu\tau}}{(\delta_2+\mu)(\delta_1+\mu+\gamma)}\left[\tau + \frac{1}{\delta_2+\mu} + \frac{1}{\delta_1+\mu+\gamma}\right] < 0 \quad \text{(negative effect)}$$

The bar chart in **Figure 2** presents the parameter values.

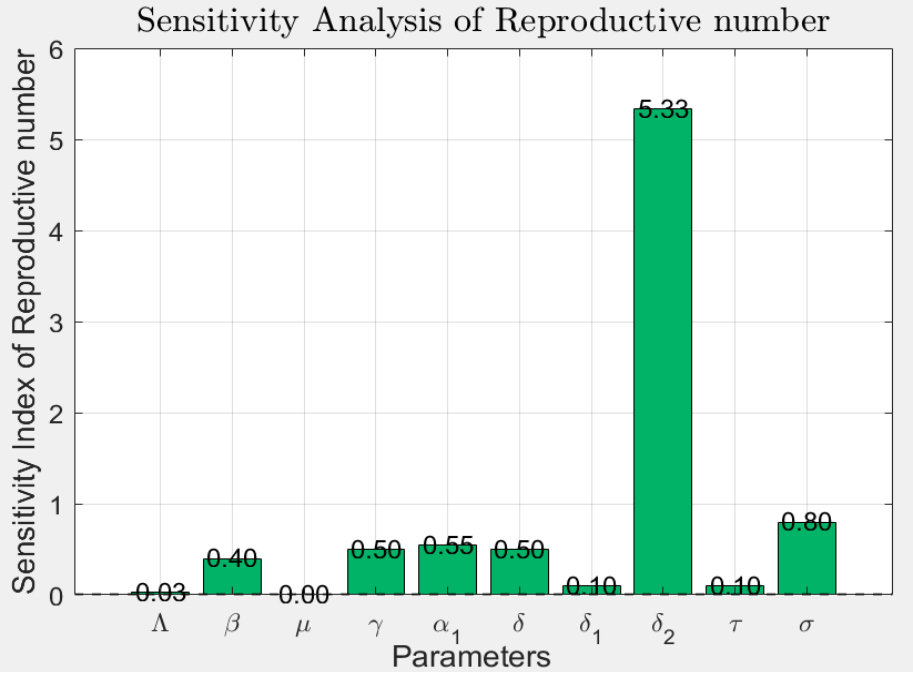

Figure 2. Parameter values.

This number depicts sensitivity analysis of the basic reproduction number $\Re_0$ of the various model parameters. It demonstrates that the δ_2 is the most sensitive parameter

(with the index of 5.33), and other parameters (Lambda, mu, and delta_1) have the least influence.

The effects of the vaccination rate δ_1 on the basic reproduction number $\mathfrak{R}_0$ are shown in the **Figure 3**. It is easy to notice that, given the increase of δ_1, the reproductive number decreases monotonously. When the number of δ_1 exceeds the susceptible, it is transformed to the vaccinated group, thus decreasing the infectious rate. As a result, large enough values of δ_1 can ensure the reduction of $\mathfrak{R}_0 < 1$, resulting in the effective elimination of the disease.

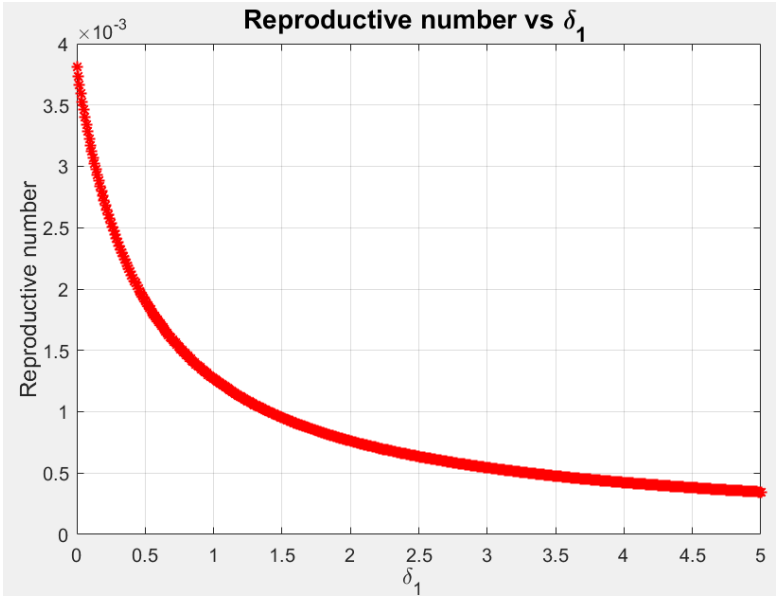

Figure 3. Relation between reproductive number and vaccination rate.

Figure 4 demonstrates that the change of Reproductive number with regard to the recovery rate γ. The higher the value of γ, the faster the infectious persons would recover resulting in a slow reduction of the Reproductive number. This demonstrates the fact that increased rates of recovery contribute to the regulation of the spread of diseases and minimization of epidemics.

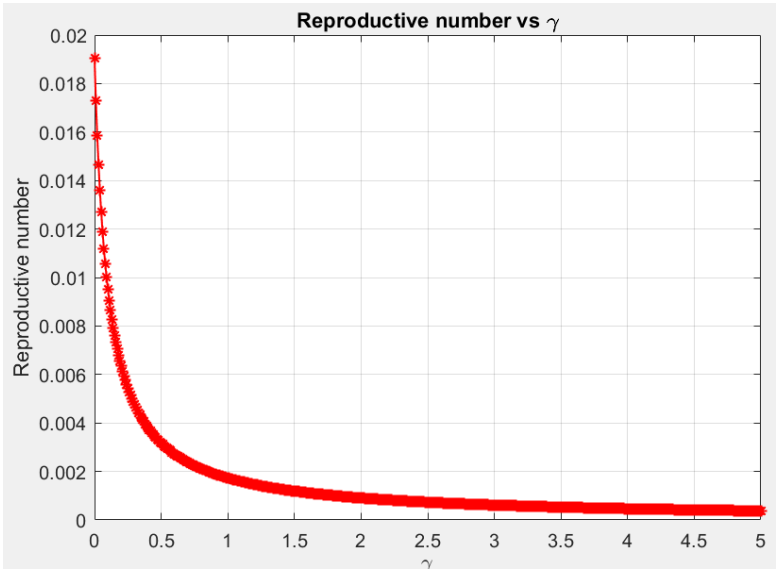

Figure 4. Relation between reproductive number and recovery rate.

Figure 5 shows that when the delay rate increases, we can see that the reproductive number decreases, so disease also decreases in the susceptible population.

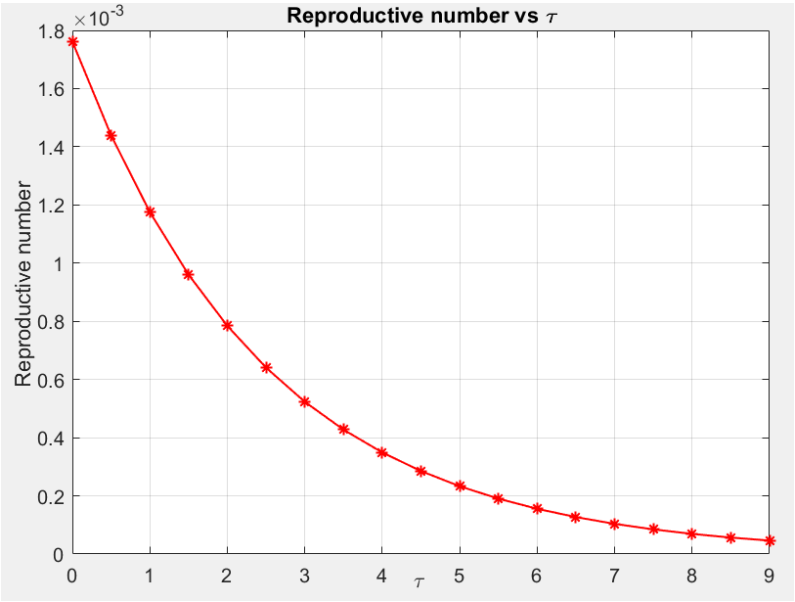

Figure 5. Relation between time delay and reproductive number.

In **Figure 6** investigate the effect of transmission and recovery rate on the reproductive number, a three-dimensional graph was generated by changing beta and gamma while the other parameter was fixed. The delay factor in the model represents the time delay in infection dynamics. The graph shows a smooth and continuous surface that describes the mathematical behavior of the reproductive number. As the transformation rate increases, the reproductive number increases, insinuating a higher risk of infection spread. On the other hand, the recovery rate increases, and the reproductive number decreases. Furthermore, the delay factor increases the overall magnitude of the reproductive number decrease. This behavior suggests that including delay into the model can effectively reduce the potential for an outbreak.

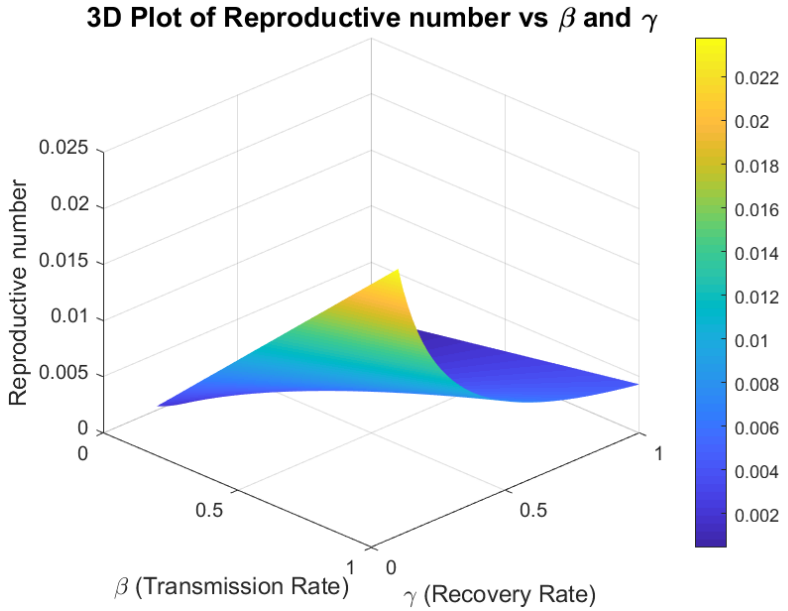

Figure 6. A 3D graph of reproductive number, Transmission rate and recovery rate.

Figure 7 shows how the reproductive number changes as the transmission rate increases for different values of susceptible population. If we increase the value of beta and S, the reproductive number becomes larger.

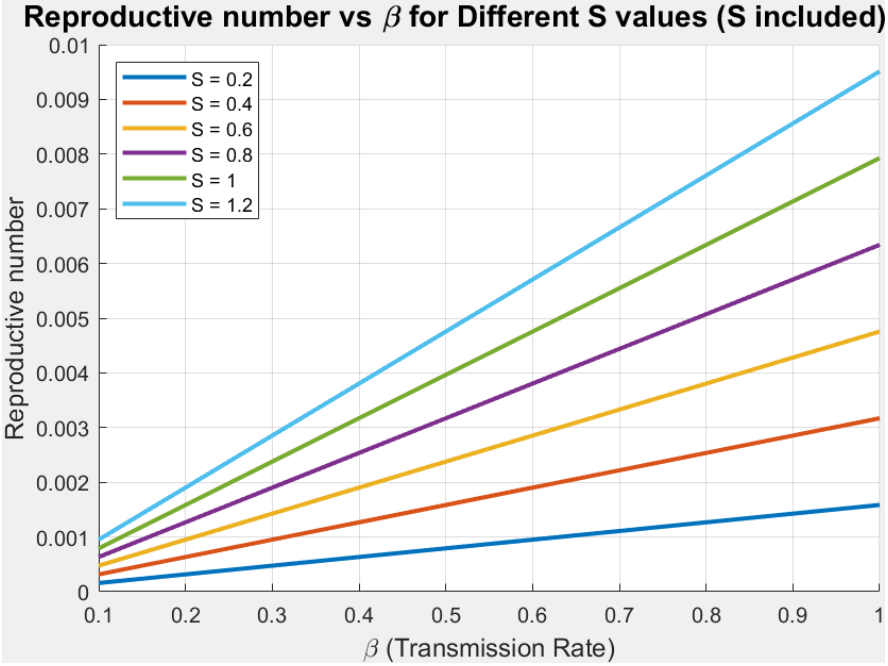

Figure 7. Relation between $\mathfrak{R}_0$ and β at different value of S.

In **Figure 8**, a set of curves was plotted to inspect how the reproductive number varies with transmission rate beta for different values of the delay factor. The results show that the reproductive number increases with beta, but its magnitude decreases as time delays become larger. By using the delay factor, the spread of the disease is reduced.

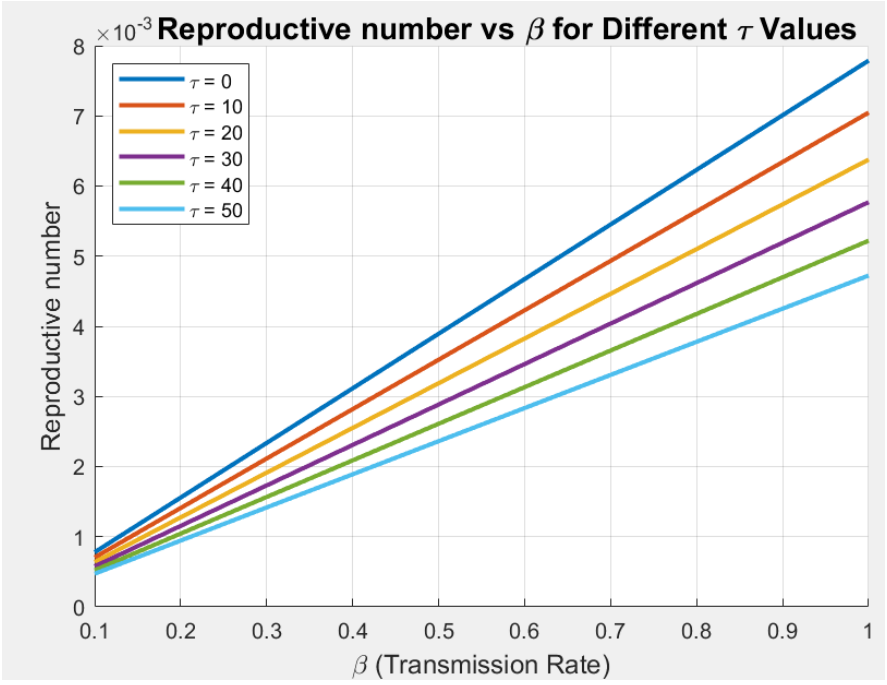

Figure 8. Relation between β and $\mathfrak{R}_0$ at different value of τ.

3. Results

3.1. Numerical simulations

This study examines two finite difference schemes for analyzing the dynamical behaviors of the system: Euler's integration and the fourth-order Runge-Kutta integration (RK-4), in conjunction with the non-standard finite difference approach (NSFD) for managing such a system.

3.1.1. Forward euler's scheme

$$S^{n+1} = S^n + h\left[\Lambda - \frac{\beta S^n I^n e^{-\mu\tau}}{1+\alpha_1 I^n} - (\delta_2+\mu)\, S^n\right], \tag{4a}$$

$$I^{n+1} = I^n + h\left[\frac{\beta S^n I^n e^{-\mu\tau}}{1+\alpha_1 I^n} - (\delta_1+\mu+\gamma)\, I^n\right], \tag{4b}$$

$$V^{n+1} = V^n + h\left[\delta_2 S^n + \delta_1 I^n - (\sigma+\mu)V^n\right], \tag{4c}$$

$$= R^n + h\left[\gamma I^n + \sigma V^n - \mu R^n\right]. \tag{4d}$$

3.1.2. Fourth order runge-kutta ($\mathbf{RK_4}$) method

$$k_1 == h\left[\Lambda - \frac{\beta S^n I^n e^{-\mu\tau}}{1+\alpha_1 I^n} - (\delta_2+\mu)\, S^n\right],$$

$$m_1 == h\left[\frac{\beta S^n I^n e^{-\mu\tau}}{1+\alpha_1 I^n} - (\delta_1+\mu+\gamma)\, I^n\right],$$

$$n_1 == h\left[\delta_2 S^n + \delta_1 I^n - (\sigma+\mu)V^n\right],$$

$$p_1 == h\left[\gamma I^n + \sigma V^n - \mu R^n\right],$$

$$k_2 = h\left[\Lambda - \frac{\beta\left(S^n + \frac{k_1}{2}\right)\left(I^n + \frac{m_1}{2}\right)e^{-\mu\tau}}{1+\alpha_1\left(I^n + \frac{m_1}{2}\right)} - (\delta_2+\mu)\left(S^n + \frac{k_1}{2}\right)\right],$$

$$m_2 = h\left[\frac{\beta\left(S^n + \frac{k_1}{2}\right)\left(I^n + \frac{m_1}{2}\right)e^{-\mu\tau}}{1+\alpha_1\left(I^n + \frac{m_1}{2}\right)} - (\delta_1+\mu+\gamma)\left(I^n + \frac{m_1}{2}\right)\right],$$

$$n_2 = h\left[\delta_2\left(S^n + \frac{k_1}{2}\right) + \delta_1\left(I^n + \frac{m_1}{2}\right) - (\sigma+\mu)\left(V^n + \frac{n_1}{2}\right)\right],$$

$$p_2 = h\left[\gamma\left(I^n + \frac{m_1}{2}\right) + \sigma\left(V^n + \frac{n_1}{2}\right) - \mu\left(R^n + \frac{p_1}{2}\right)\right],$$

$$k_3 = h\left[\Lambda - \frac{\beta\left(S^n + \frac{k_2}{2}\right)\left(I^n + \frac{m_2}{2}\right)e^{-\mu\tau}}{1+\alpha_1\left(I^n + \frac{m_2}{2}\right)} - (\delta_2+\mu)\left(S^n + \frac{k_2}{2}\right)\right],$$

$$m_3 == h\left[\frac{\beta\left(S^n + \frac{k_2}{2}\right)\left(I^n + \frac{m_2}{2}\right)e^{-\mu\tau}}{1+\alpha_1\left(I^n + \frac{m_2}{2}\right)} - (\delta_1+\mu+\gamma)\left(I^n + \frac{m_2}{2}\right)\right],$$

$$n_3 = h\left[\delta_2\left(S^n + \frac{k_2}{2}\right) + \delta_1\left(I^n + \frac{m_2}{2}\right) - (\sigma+\mu)\left(V^n + \frac{n_2}{2}\right)\right],$$

$$p_3 = h\left[\gamma\left(I^n + \frac{m_2}{2}\right) + \sigma\left(V^n + \frac{n_2}{2}\right) - \mu\left(R^n + \frac{p_2}{2}\right)\right],$$

$$k_4 == h\left[\Lambda - \frac{\beta\left(S^n + k_3\right)\left(I^n + m_3\right)e^{-\mu\tau}}{1 + \alpha_1\left(I^n + m_3\right)} - \left(\delta_2 + \mu\right)\left(S^n + k_3\right)\right],$$

$$m_4 == h\left[\frac{\beta\left(S^n + k_3\right)\left(I^n + m_3\right)e^{-\mu\tau}}{1 + \alpha_1\left(I^n + m_3\right)} - \left(\delta_1 + \mu + \gamma\right)\left(I^n + m_3\right)\right],$$

$$n_4 = h\left[\delta_2\left(S^n + k_3\right) + \delta_1\left(I^n + m_3\right) - \left(\sigma + \mu\right)\left(V^n + n_3\right)\right],$$

$$p_4 == h\left[\gamma\left(I^n + m_3\right) + \sigma\left(V^n + n_3\right) - \mu\left(R^n + p_3\right)\right],$$

Thus, the ultimate results are,

$$S^{n+1} = S^n + \frac{1}{6}\left[k_1 + 2k_2 + 2k_3 + k_4\right], \tag{5a}$$

$$I^{n+1} = I^n + \frac{1}{6}\left[m_1 + 2m_2 + 2m_3 + m_4\right], \tag{5b}$$

$$V^{n+1} = V^n + \frac{1}{6}\left[n_1 + 2n_2 + 2n_3 + n_4\right], \tag{5c}$$

$$R^{n+1} = R^n + \frac{1}{6}\left[p_1 + 2p_2 + 2p_3 + p_4\right]. \tag{5d}$$

3.1.3. Non-standard finite difference method

In this part, we will look at the stability of the non-standard finite difference method of the SIVR model at the disease-free equilibrium point.

$$\begin{aligned}
S^{n+1} &= \frac{S^n + h\Lambda}{1 + h\left(\delta_2 + \mu\right) + \frac{h\beta I^n e^{-\mu\tau}}{1+\alpha_1 I^n}}. \\
I^{n+1} &= \frac{I^n}{\left(1 + h\left(\delta_1 + \mu + \gamma\right)\right)} + \frac{h\beta S^n I^n e^{-\mu\tau}}{\left(1 + \alpha_1 I^n\right)\left(1 + h\left(\delta_1 + \mu + \gamma\right)\right)}. \\
V^{n+1} &= \frac{V^n + h\delta_2 S^n + h\delta_1 I^n}{\left(1 + h\sigma + h\mu\right)}. \\
R^{n+1} &= \frac{R^n + h\gamma I^n + h\sigma V^n}{\left(1 + h\mu\right)}.
\end{aligned} \tag{6}$$

3.2. Stability analysis of NSFD scheme

By taking the NSFD equation, and this equation is equal to other variables.

$$\begin{aligned}
C &= \frac{S^n + h\Lambda}{1 + h\left(\delta_2 + \mu\right) + \frac{h\beta I^n e^{-\mu\tau}}{1+\alpha_1 I^n}} \\
D &= \frac{I^n}{\left(1 + h\left(\delta_1 + \mu + \gamma\right)\right)} + \frac{h\beta S^n I^n e^{-\mu\tau}}{\left(1 + \alpha_1 I^n\right)\left(1 + h\left(\delta_1 + \mu + \gamma\right)\right)} \\
E &= \frac{V^n + h\delta_2 S^n + h\delta_1 I^n}{\left(1 + h\sigma + h\mu\right)} \\
F &= \frac{R^n + h\gamma I^n + h\sigma V^n}{\left(1 + h\mu\right)}
\end{aligned}$$

By taking the partial derivative of C, D, E, and F with respect to model parameter. After this by putting the value of disease-free point (DFP). we get the matrix J.

$$J=\begin{bmatrix} \frac{1}{1+h(\delta_2+\mu)} & -\frac{h\beta e^{-\mu\tau}(\Lambda+h\Lambda(\delta_2+\mu))}{(\delta_2+\mu)(1+h(\delta_2+\mu))^2} & 0 & 0 \\ 0 & \frac{1}{1+h(\delta_1+\mu+\gamma)}+\frac{h\beta\Lambda e^{-\mu\tau}}{(\delta_2+\mu)(1+h(\delta_1+\mu+\gamma))} & 0 & 0 \\ \frac{h\delta_2}{1+h\sigma+h\mu} & \frac{h\delta_1}{1+h\sigma+h\mu} & \frac{1}{1+h\sigma+h\mu} & 0 \\ 0 & \frac{h\gamma}{1+h\mu} & \frac{h\sigma}{1+h\mu} & \frac{1}{1+h\mu} \end{bmatrix}$$

For this Jacobi matrix we obtained that all eigen values are less than one so system is stable.

3.3. Consistency analysis

The consistency analysis of our numerical scheme is conducted using Taylor's series expansion. Firstly, we select the Susceptible equation from the numerical integration model and apply Taylor's series expansion on S_{n+1}.

$$S^{n+1}=S^n+h\frac{dS}{dt}+\frac{h^2}{2!}\frac{d^2S}{dt^2}+\frac{h^3}{3!}\frac{d^3S}{dt^3}+\dots$$

From above equation we get,

$$S^{n+1}\left(1+h\left(\delta_2+\mu\right)+\frac{h\beta I^n e^{-\mu\tau}}{1+\alpha_1 I^n}\right)=S^n+h\Lambda,$$

put the value of S_{n+1}

$$\left(S^n+h\frac{dS^n}{dt}+\frac{h^2}{2!}\frac{d^2S^n}{dt^2}+\frac{h^3}{3!}\frac{d^3S^n}{dt^3}+...\right)\left(1+h\left(\delta_2+\mu\right)+\frac{\beta I^n e^{-\mu\tau}}{1+\alpha_1 I^n}\right)=S^n+h\Lambda,$$

$$S^n+S^n h\left(\delta_2+\mu\right)+hS^n\frac{\beta I^n e^{-\mu\tau}}{1+\alpha_1 I^n}+h\frac{dS^n}{dt}+h^2\frac{dS^n}{dt}\left(\delta_2+\mu\right)+h^2\frac{dS^n}{dt}\frac{\beta I^n e^{-\mu\tau}}{1+\alpha_1 I^n}$$
$$+\left(\frac{h^2}{2!}\frac{d^2S^n}{dt^2}+\frac{h^3}{3!}\frac{d^3S^n}{dt^3}+...\right)\left(1+h\left(\delta_2+\mu\right)+\frac{\beta I^n e^{-\mu\tau}}{1+\alpha_1 I^n}\right)=S^n+h\Lambda,$$

After Simplification,

$$h\left(S^n\left(\delta_2+\mu\right)+S^n\frac{\beta I^n e^{-\mu\tau}}{1+\alpha_1 I^n}\right)+\frac{dS^n}{dt}+h\frac{dS^n}{dt}\left(\delta_2+\mu\right)+h\frac{dS^n}{dt}\left(\frac{\beta I^n e^{-\mu\tau}}{1+\alpha_1 I^n}\right)$$
$$+\left(\frac{h^2}{2!}\frac{d^2S^n}{dt^2}+\frac{h^3}{3!}\frac{d^3S^n}{dt^3}+...\right)\left(1+h\left(\delta_2+\mu\right)+\frac{\beta I^n e^{-\mu\tau}}{1+\alpha_1 I^n}\right)=h\Lambda,$$

After cancellation,

$$\left(S^n\left(\delta_2+\mu\right)+S^n\frac{\beta I^n e^{-\mu\tau}}{1+\alpha_1 I^n}\right)+\frac{dS^n}{dt}+h\frac{dS^n}{dt}\left(\delta_2+\mu\right)+h\frac{dS^n}{dt}\left(\frac{\beta I^n e^{-\mu\tau}}{1+\alpha_1 I^n}\right)$$
$$+\left(\frac{h^2}{2!}\frac{d^2S^n}{dt^2}+\frac{h^3}{3!}\frac{d^3S^n}{dt^3}+...\right)\left(1+h\left(\delta_2+\mu\right)+\frac{\beta I^n e^{-\mu\tau}}{1+\alpha_1 I^n}\right)=\Lambda,$$

By applying h $\to 0$, we get

$$\left(S^n\left(\delta_2+\mu\right)+S^n\frac{\beta I^n e^{-\mu\tau}}{1+\alpha_1 I^n}\right)+\frac{dS^n}{dt}=\Lambda,$$

Rearrange the equation.

$$\frac{dS^n}{dt}=\Lambda-S^n\left(\delta_2+\mu\right)-\frac{\beta I^n S^n e^{-\mu\tau}}{1+\alpha_1 I^n}.$$

The above equation show that our equation is consistent with the model equation (1). After that we apply the same process on I^{n+1}, we get final equation

$$\frac{dI^n}{dt}=\frac{\beta S^n I^n e^{-\mu\tau}}{1+\alpha I^n}-\left(\delta_1+\mu+\gamma\right)I^n.$$

Since the same process apply on V^{n+1}, we get

$$\frac{dV^n}{dt}=\delta_2 S^n+\delta_1 I^n-(\sigma+\mu)V^n.$$

Since the same process apply on R^{n+1}, we get

$$\frac{dR^n}{dt}=\gamma I^n+\sigma V^n-\mu R^n.$$

Hence, these equations show that our NSFD scheme is consistent with this system.

3.4. Graphical analysis

This section is devoted for investigating the key properties of the simulated graphs against the set of parametric values as mentioned in **Table 1**. Further, these graphs are plotted at the disease free and endemicpoints.

Case 1(a): First of all, we can compare the Euler method and the NSFD method at step size $h=2.8$ in **Figure 9**; at that point in disease-free equilibrium, Euler shows oscillation and NSFD shows convergence. So, we can conclude that NSFD is more reliable and sufficient as compared to the Euler method. In disease free equilibrium the reproductive number $\mathfrak{R}_0<1$.

Case 1(b): We can compare the Euler method and the NSFD method at step size $h=5.5$ in **Figure 10**; at that point in disease-free equilibrium, Euler show divergence, but NSFD shows convergence. So, we can conclude that NSFD is more reliable and sufficient as compared to the Euler method. In disease free equilibrium the reproductive number $\mathfrak{R}_0<1$.

Case 1(c): In the **Figure 11** we can again compare the Euler and NSFD methods, but this time Euler shows divergence at the endemic equilibrium point with a step size $h=0.3$, and NSFD shows convergence at that point. In endemic equilibrium the reproductive number $\mathfrak{R}_0>1$.

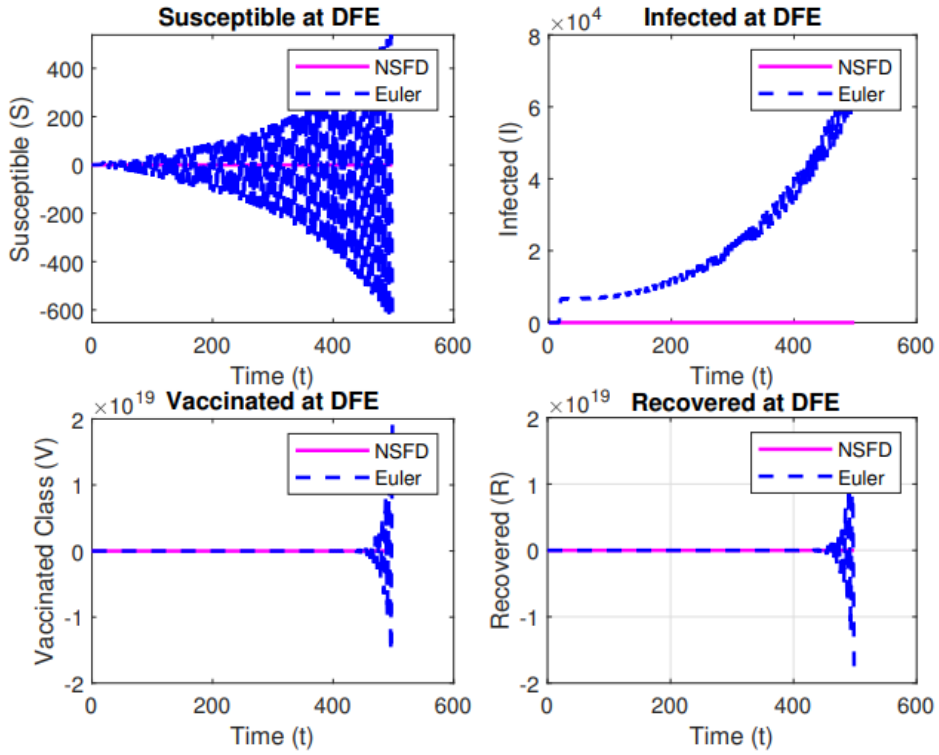

Figure 9. Comparison of Euler and NSFD at h = 2.8.

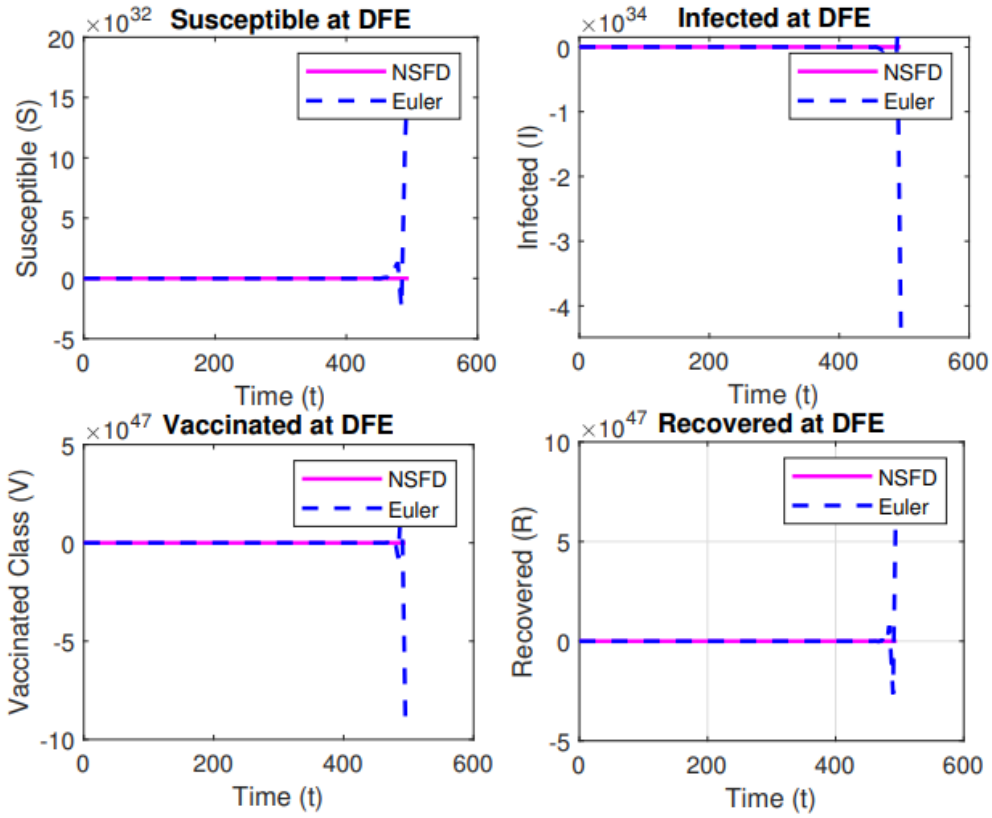

Figure 10. Comparison of Euler and NSFD at h = 5.5.

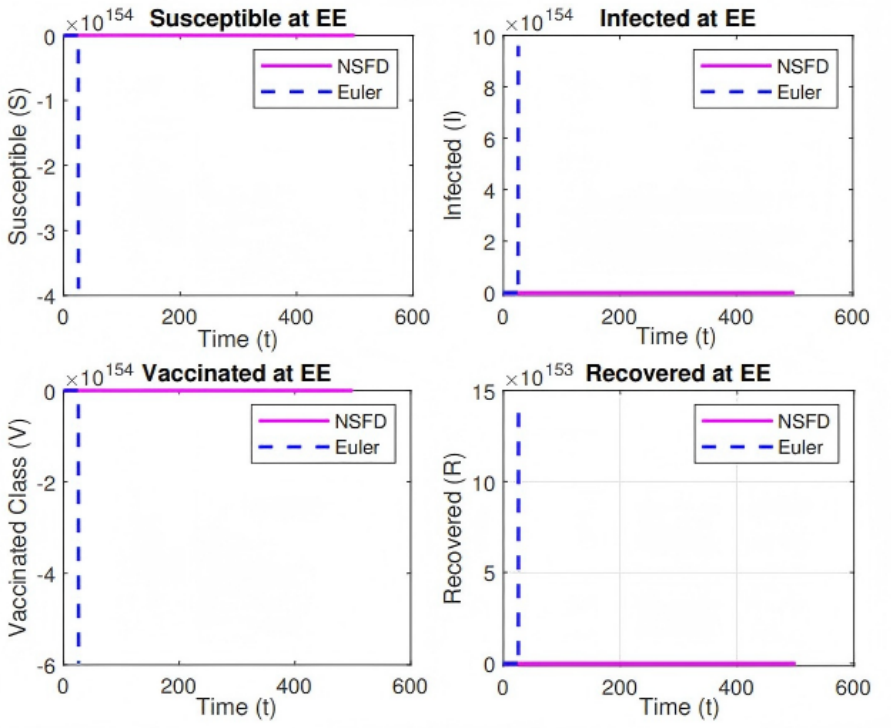

Figure 11. Comparison of Euler and NSFD at h = 0.3.

Case 2(a): Second, we employed the Runge-Kutta technique at **Figure 12**; the simulation of the disease-free equilibrium sites showed oscillations and negative behavior at step size h = 0.6 and NSFD shows convergence at the disease-free equilibrium points. In disease-free equilibrium the reproductive number $\mathfrak{R}_0 < 1$.

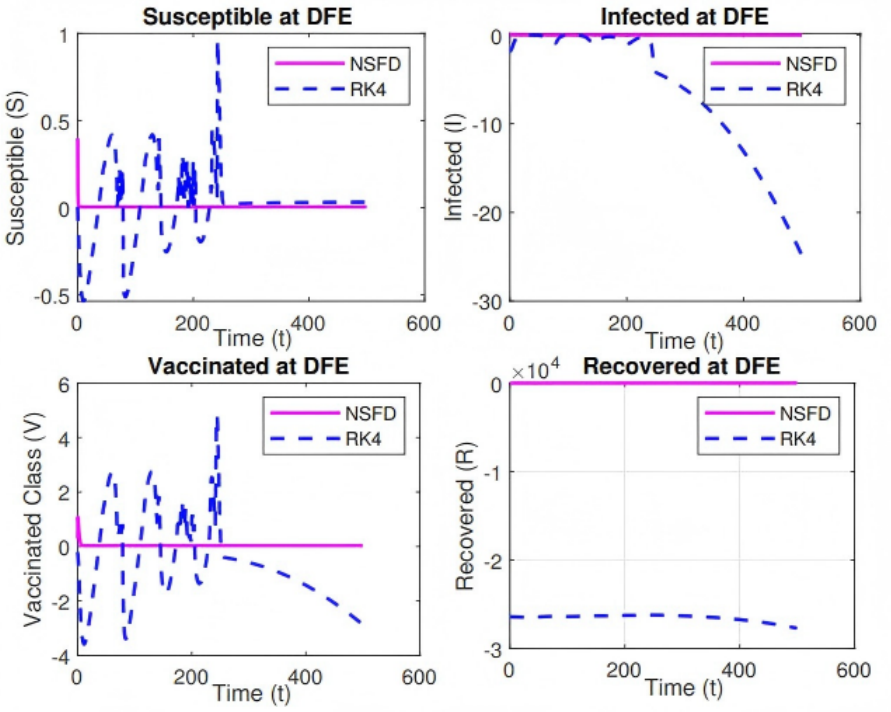

Figure 12. Comparison of Rk_4 and NSFD at h = 0.6.

Case 2(b): We employed the Runge-Kutta technique at **Figure 13**; the simulation of the disease-free equilibrium sites showed divergence at step size h = 4.4 as shown

in the figures, but NSFD shows convergence at the disease-free equilibrium points. In disease-free equilibrium the reproductive number $\mathfrak{R}_0 < 1$.

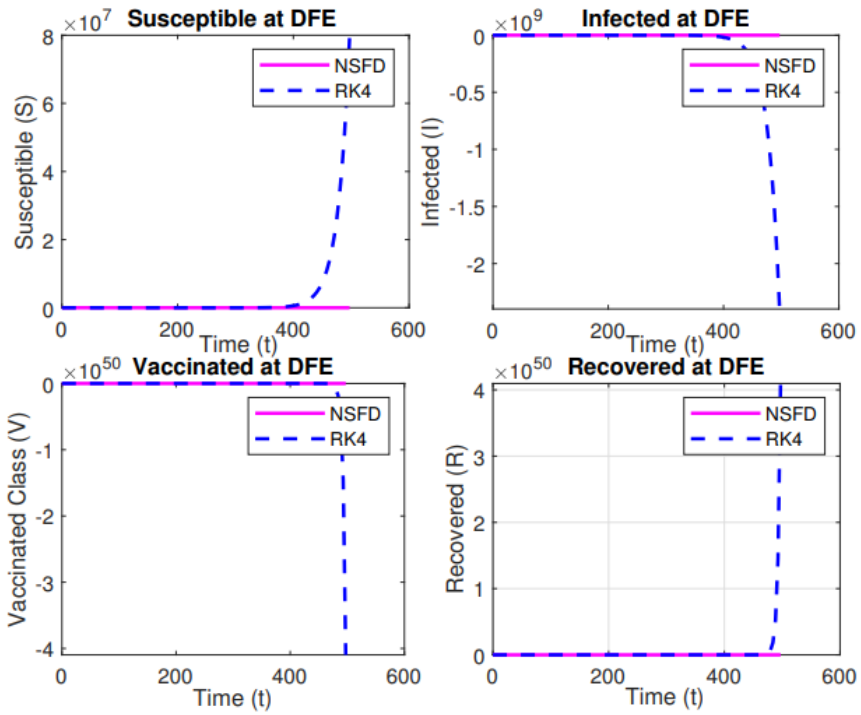

Figure 13. Comparison of Rk_4 and NSFD at h = 4.4.

Case 2(c): In this **Figure 14** we can compare the Runge-Kutta method and NSFD method at step size h = 4.4; in the endemic equilibrium at that point Runge-Kutta shows divergence and NSFD shows convergence and positive behavior. In endemic equilibrium the reproductive number $\mathfrak{R}_0 > 1$.

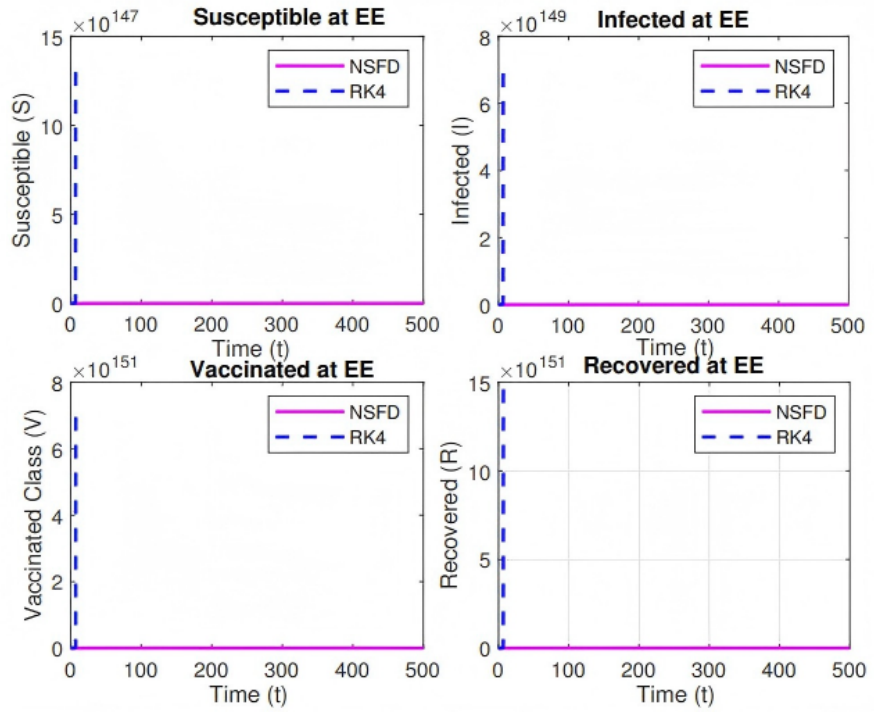

Figure 14. Comparison of Rk_4 and NSFD at h = 4.4.

4. Conclusions

This mathematical research paper offers an accurate and dependable corona virus pandemic model, followed by numerical findings obtained using a non-standard finite difference technique. It has been shown that the delay factor has a significant impact on the spread of coronavirus disease in people. Equilibrium calculations are performed for the delay pandemic model. The local and global stability of the Disease-Free (DFE) and Endemic (EE) points are also examined. We verified the model's uniqueness and existence, ensuring that it performs reliably and can be trusted for practical or theoretical purposes. This technique is valuable because the NSFD strategy preserves the most important features of the coronavirus pandemic scenario. Despite this, our consistency investigation showed that the method accurately approximates the real result. Additionally, the fourth-order (RK-4) and Euler methods were used to assess the NSFD technique. The simulations demonstrate that even at incredibly small step sizes, both conventional and well-known methods fall short in producing reliable and accurate results. Consequently, among the conventional finite difference approaches, the proposed method is one of the best choices. Though, the study is restricted by the fact that it only incorporates one delay parameter and does not consider the spatial heterogeneity or stochastic. The model can be expanded to include various delays, uncertainty, and spatial effects in the future to reflect the dynamics of the epidemic in the real world.

Author contributions: AA: Methodology, Formal Analysis, Investigation, Data Curation, Writing—Original Draft. MUA: Methodology, Formal Analysis, Investigation, Data Curation, Writing—Original Draft. SZ: Conceptualization, Methodology, Formal Analysis, Investigation, Data Curation, Writing—Original Draft, Visualization. BC: Supervision, Project Administration, Funding Acquisition, Methodology, Data Curation, Formal Analysis. MR: Methodology, Formal Analysis, Investigation, Data Curation, Writing—Original Draft. AK: Supervision, Project Administration, Data Curation, Formal Analysis. AS: Investigation, Data Curation. All authors have read and agreed to the published version of the manuscript.

Acknowledgment: We thanks to The Advance in Differential Equations and Control Process for financial support.

Conflict of interest: The authors declare that there is no conflict of interest.

References

1. Kumar N, Tyagi R. Various impacts of COVID-19 on environmental pollution. International Journal of Human Capital in Urban Management. 2021; 6(1). doi: 10.22034/IJHCUM.2021.01.01
2. Saleem S, Rafiq M, Ahmed N, et al. Fractional epidemic model of coronavirus disease with vaccination and crowding effects. Scientific Reports. 2024; 14(1): 8157. doi: 10.1038/s41598-024-58192-7
3. McCloskey B, Heymann DL. SARS to novel coronavirus – old lessons and new lessons. Epidemiology and Infection. 2020; 148: e22. doi: 10.1017/S0950268820000254
4. Saha S, Samanta GP. Modelling the role of optimal social distancing on disease prevalence of COVID-19 epidemic. International Journal of Dynamics and Control. 2021; 9(3): 1053–1077. doi: 10.1007/s40435-020-00721-z

5. Shereen MA, Khan S, Kazmi A, et al. COVID-19 infection: emergence, transmission, and characteristics of human coronaviruses. Journal of Advanced Research. 2020; 24: 91–98. doi: 10.1016/j.jare.2020.03.005
6. Zeb S, Bilal M, Rafiq M, et al. Structure preserving numerical analysis of HIV/AIDS epidemic model. International Journal of Mathematical Modelling and Numerical Optimisation. 2025; 15(4): 293–323. doi: 10.1504/IJMMNO.2025.149421
7. Sohrabi C, Alsafi Z, O'Neill N, et al. World health organization declares global emergency: a review of the 2019 novel coronavirus (COVID-19). International Journal of Surgery. 2020; 76: 71–76. doi: 10.1016/j.ijsu.2020.02.034
8. Baud D, Qi X, Nielsen-Saines K, et al. Real estimates of mortality following COVID-19 infection. The Lancet Infectious Diseases. 2020; 20(7): 773. doi: 10.1016/S1473-3099(20)30195-X
9. Alinia-Ahandani E, Sheydaei M. Overview of the introduction to the new coronavirus (Covid19): a review. Journal of Medical and Biological Science Research. 2020; 6(2): 14–20. doi: 10.36630/jmbsr_20005
10. Shim E, Tariq A, Choi W, et al. Transmission potential and severity of COVID-19 in south korea. International Journal of Infectious Diseases. 2020; 93: 339–344. doi: 10.1016/j.ijid.2020.03.031
11. Ahmed I, Modu GU, Yusuf A, et al. A mathematical model of coronavirus disease (COVID-19) containing asymptomatic and symptomatic classes. Results in Physics. 2021; 21: 103776. doi: 10.1016/j.rinp.2020.103776
12. Hassan MN, Mahmud MdS, Nipa KF, et al. Mathematical modeling and COVID-19 forecast in texas, USA: a prediction model analysis and the probability of disease outbreak. Disaster Medicine and Public Health Preparedness. 2023; 17: e19. doi: 10.1017/dmp.2021.151
13. Alqarni MS, Alghamdi M, Muhammad T, et al. Mathematical modeling for novel coronavirus (COVID -19) and control. Numerical Methods for Partial Differential Equations. 2022; 38(4): 760–776. doi: 10.1002/num.22695
14. Savi PV, Savi MA, Borges B. A mathematical description of the dynamics of coronavirus disease 2019 (COVID-19): a case study of brazil. Computational and Mathematical Methods in Medicine. 2020; 2020: 1–8. doi: 10.1155/2020/9017157
15. Tiwari V, Deyal N, Bisht NS. Mathematical modeling based study and prediction of COVID-19 epidemic dissemination under the impact of lockdown in india. Frontiers in Physics. 2020; 8: 586899. doi: 10.3389/fphy.2020.586899
16. Warbhe SD, Lamba NK, Deshmukh KC. Impact of COVID-19: a mathematical model. Journal of Interdisciplinary Mathematics. 2021; 24(1): 77–87. doi: 10.1080/09720502.2020.1833444
17. AlArjani A, Nasseef MT, Kamal SM, et al. Application of mathematical modeling in prediction of COVID-19 transmission dynamics. Arabian Journal for Science and Engineering. 2022; 47(8): 10163–10186. doi: 10.1007/s13369-021-06419-4
18. Ndaïrou F, Area I, Nieto JJ, et al. Mathematical modeling of COVID-19 transmission dynamics with a case study of wuhan. Chaos, Solitons & Fractals. 2020; 135: 109846. doi: 10.1016/j.chaos.2020.109846
19. Saha S, Samanta GP, Nieto JJ. Epidemic model of COVID-19 outbreak by inducing behavioural response in population. Nonlinear Dynamics. 2020; 102(1): 455–487. doi: 10.1007/s11071-020-05896-w
20. Zeb S, Mohd Yatim SA, Ahmad A, et al. Numerical modelling of SEIR on two-dose vaccination against the rubella virus. Malaysian Journal of Fundamental and Applied Sciences. 2025; 21(1): 1577–1601. doi: 10.11113/mjfas.v21n1.3713
21. Rezaei N. Correction to: integrated science of global epidemics. In: Rezaei N. (editor). Integrated Science of Global Epidemics, Integrated Science. Springer International Publishing; 2023. pp. C1–C1. doi: 10.1007/978-3-031-17778-1_29
22. Kubra KT, Ali R, Alqahtani RT, et al. Analysis and comparative study of a deterministic mathematical model of SARS-COV-2 with fractal-fractional operators: a case study. Scientific Reports. 2024; 14(1): 6431. doi: 10.1038/s41598-024-56557-6
23. Ullah S, Mohd Nor NH, Daud H, et al. Spatial cluster analysis of COVID-19 in malaysia (mar-sep, 2020). Geospatial Health. 2021; 16(1). doi: 10.4081/gh.2021.961
24. Azmi PAR, Abidin AWZ, Mutalib S, et al. Sentiment analysis on MySejahtera application during COVID-19 pandemic. In: Proceedings of the 2022 3rd International Conference on Artificial Intelligence and Data Sciences (AiDAS); 7 September 2022; IPOH, Malaysia; pp. 215–220. doi: 10.1109/AiDAS56890.2022.9918748
25. Mutalib S, Pungut SNM, Abidin AWZ, et al. Development of regression models for COVID-19 trends in malaysia. Wseas Transactions On Information Science And Applications. 2023; 20: 398–408. doi: 10.37394/23209.2023.20.42
26. Ahmed A, Salam B, Mohammad M, et al. Analysis coronavirus disease (COVID-19) model using numerical approaches and logistic model. AIMS Bioengineering. 2020; 7(3): 130–146. doi: 10.3934/bioeng.2020013

27. Ramzan Y, Riaz A, Guedri K, et al. A nonlinear optimization framework for a Lassa fever model capturing zoogenic transmission and disability risks. The European Physical Journal Plus. 2025; 140(10): 975. doi: 10.1140/epjp/s13360-025-06902-z
28. Ramzan Y, Guedri K, Awan AU, et al. Modeling gonorrhea and HIV coinfection with predictive analytics for disability and mortality risks. Scientific Reports. 2025; 15(1): 32983. doi: 10.1038/s41598-025-16601-5
29. Cangiotti N, Capolli M, Sensi M, et al. A survey on Lyapunov functions for epidemic compartmental models. Bollettino dell'Unione Matematica Italiana. 2024; 17(2): 241–257. doi: 10.1007/s40574-023-00368-6
30. Ramzan Y, Fadhl BM, Niazai S, et al. Decoding the transmission and subsequent disability risks of rabineurodeficiency syndrome without recuperation. Scientific Reports. 2025; 15(1): 17322. doi: 10.1038/s41598-025-01066-3
31. Ramzan Y, Alzubadi H, Awan AU, et al. A mathematical lens on the zoonotic transmission of lassa virus infections leading to disabilities in severe cases. Mathematical and Computational Applications. 2024; 29(6): 102. doi: 10.3390/mca29060102